

Interstitial Glucose Kinetics in Subjects With Type 1 Diabetes Under Physiologic Conditions

Malgorzata E. Wilinska, Manfred Bodenlenz, Ludovic J. Chassin, Helga C. Schaller, Lukas A. Schaupp, Thomas R. Pieber, and Roman Hovorka

We investigated the dynamic relationship between interstitial glucose (IG) in the subcutaneous adipose tissue and plasma glucose (PG) during physiologic conditions in type 1 diabetes mellitus (T1DM). Nine subjects with T1DM (5/4 M/F; age, 33 ± 13 years; body mass index, 26.6 ± 4.3 kg/m²; glycosylated hemoglobin [HbA_{1c}], $8.6\% \pm 0.9\%$; mean \pm SD) treated by continuous subcutaneous insulin infusion (CSII) with insulin lispro were studied over 12 hours after a standard meal (40 g carbohydrate [CHO]) and prandial insulin. IG was measured by open flow microperfusion. Nine compartment models were postulated to account for temporal variations in the IG/PG ratio. The models differed in the inclusion of physiologically motivated alterations of pathways entering/leaving the IG compartment in the adipose tissue. The best model included zero order (constant) glucose disposal from the interstitial fluid (ISF) and insulin-stimulated glucose transfer from plasma to the ISF. The former effect is expressed by a positive association between the IG/PG ratio and PG, eg, a decrease in PG from 9 to 3.3 mmol/L lowers the IG/PG ratio by 0.1. The latter effect results in the IG/PG ratio to be increased by 0.03 per 10 mU/L of plasma insulin. We were not able to detect the stimulatory effect of insulin on glucose disappearance from the ISF. In conclusion, we developed and quantified a model of IG kinetics in the adipose tissue applicable to physiologic conditions in subjects with T1DM.

© 2004 Elsevier Inc. All rights reserved.

GLUCOSE MONITORING IS an essential part of diabetes management. In type 1 diabetes mellitus (T1DM), where fluctuations of blood glucose levels can be very high and unpredictable, a high frequency of monitoring is recommended. Even when the measurements are frequent, typically before and after meals, clinically significant glucose fluctuations and hypoglycemia may not be detected. To overcome this problem, methods for continuous glucose monitoring have been introduced in recent years.

Noninvasive methods of glucose sensing, such as near-infrared spectroscopy,¹ are the preferred choice. Such methods, however, face considerable problems of spectral overlap and optical changes with varying blood volume and temperature² and are still in their early stages of development. Other possible techniques involve subcutaneous implantation of a glucose sensor or collecting the interstitial fluid (ISF) for glucose measurement ex vivo using an extracorporeal sensor. Variety of techniques used for ISF collection includes ultrafiltration,³ the wick technique,⁴ microdialysis,⁵ transdermal extraction,⁶ and open flow microperfusion (OFM).⁷ Microdialysis and OFM have been shown to be suitable for continuous ex vivo on-line glucose monitoring.^{5,7,8}

An important issue, when subcutaneous glucose sensing is

considered, is the difference between the blood glucose concentration, a reference value for all clinical decision making, and the glucose concentration in the ISF.

Studies evaluating the relationship between plasma glucose (PG) and interstitial glucose (IG) have provided conflicting results. Investigators demonstrated the presence of a gradient between PG and IG of a varying magnitude from 20%⁹ to 110%.¹⁰ An equilibration time delay between PG and IG has been reported in the range from 2.3 minutes¹¹ to 45 minutes.¹² The possible reasons for the highly variable results include a variety of techniques and methods used, differences in subjects/species, as well as experimental conditions, eg, glucose/insulin clamp. Most of those studies have demonstrated not a constant, but changing interstitial to plasma glucose gradient (the IG/PG ratio). This implies that the IG-PG relationship is not simple. A more detailed understanding is required if subcutaneous glucose sensing is to become an even more accurate surrogate for PG measurements.

The understanding of the gradient and the dynamics of the relationship between IG and PG depend on the understanding and quantification of the physiologic processes in the ISF compartment surrounding the adipose tissue. PG is separated from the IG by a capillary wall (see Fig 1). Hence changes in IG are related to changes in PG by the rate of diffusion across the capillary wall and by the rate of glucose removal from the ISF. The removal represents the uptake by adipose tissue immediately surrounding the sampling probe and transport back to the plasma. Rebrin et al¹³ argue that if the uptake by adipocytes is negligible, PG and IG should equilibrate in steady-state conditions. If, however, the uptake is not negligible, then a steady-state gradient will exist between PG and IG concentration. Assuming that glucose uptake by adipose tissue is sensitive to insulin, an increase in insulin concentration should result in an increased uptake of glucose by adipocytes, and therefore, an increase in plasma to interstitial glucose gradient.

The existence of the so called “push-pull” phenomenon has been suggested in the literature. The phenomenon is thought to

From the Diabetes Modelling Group, Department of Paediatrics, University of Cambridge, Addenbrooke's Hospital, Cambridge, UK; Department of Internal Medicine, Diabetes and Metabolism, Karl Franzens University, Graz; and the Department of Biophysics, Institute of Biomedical Engineering, University of Technology, Graz, Austria.

Submitted February 9, 2004; accepted May 3, 2004.

Supported by the 5th EC Framework Programme, Grant No. IST-1999-14027 (ADICOL).

Address reprint requests to Roman Hovorka, PhD, Diabetes Modelling Group, Department of Paediatrics, University of Cambridge, Box 116, Addenbrooke's Hospital, Hills Rd, Cambridge CB2 2QQ, UK.

© 2004 Elsevier Inc. All rights reserved.

0026-0495/04/5311-0042\$30.00/0

doi:10.1016/j.metabol.2004.05.014

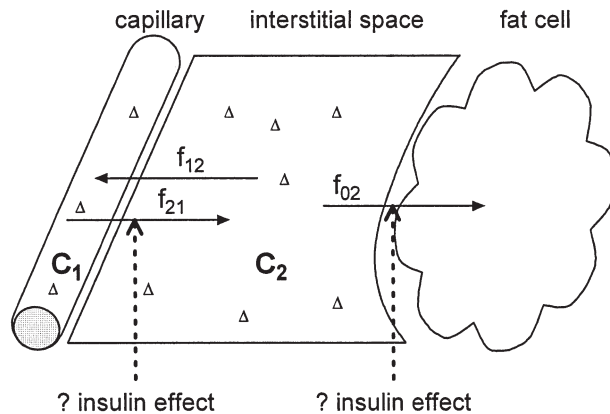


Fig 1. Conceptual description of IG kinetics; C_1 and C_2 represent glucose concentration in the plasma and the ISF, respectively, f_{02} represents glucose flux from the ISF into the fat cell, f_{12} and f_{21} represent glucose fluxes from the ISF into the plasma and from the plasma to the ISF, respectively. Glucose molecule is represented by Δ .

be caused by insulin-stimulated glucose removal from the ISF (insulin effect on flux f_{02} in Fig 1). Because the decrease in glucose is presumed to originate in the ISF with glucose being pulled from the ISF, the changes in IG should precede the changes in PG. Conversely, as the increase in glucose is assumed to originate in plasma with glucose being pushed into the ISF, the changes in IG should lag behind the changes in PG.

Several investigators claim to have detected the push-pull phenomenon,^{11,14,15} Rebrin et al,¹³ in their study in nondiabetic dogs, disputed its existence showing that insulin does not appear to have any effect on glucose removal from the ISF in adipose tissue. It was suggested that the effect of IG being pulled out from the ISF surrounding the probe could possibly be counteracted by the changes in IG originating in the areas distant from the probe/sensor.

The majority of previous studies used glucose clamps achieving nonphysiologic conditions and/or were performed in animals or nondiabetic humans. As subcutaneous glucose sensing has its main application in subjects with T1DM during normal physiologic conditions, the present study aimed to describe the IG-PG relationship during and after meal in T1DM. The OFM technique was used to measure IG. A compartment modelling approach was adopted to postulate competing models and to represent mechanisms explaining temporal variations in the IG/PD ratio. Using selection criteria based on the principle of parsimony, a model was selected which best explained experimental data while attaining physiologic plausibility.

SUBJECTS AND METHODS

Subjects and Experimental Protocol

Nine subjects with T1DM (5/4 M/F, age 33 ± 13 years; body mass index, 26.6 ± 4.3 kg/m²; glycosylated haemoglobin [HbA_{1c}] $8.6\% \pm 0.9\%$; mean \pm SD) treated by continuous subcutaneous insulin infusion (CSII) with insulin lispro participated in the study. All participants provided written informed consent and the study was approved by the

local ethical committee. The subjects followed their standard diet and insulin regimen prior to the study.

Six subjects (subjects 1 to 6) were studied after an overnight fast (start of the study at 8 AM) and 3 subjects (subjects 7 to 9) were studied at postprandial conditions (start of the study at 7 PM). The subjects were admitted to the University Hospital, University of Graz, 1 hour prior to and remained supine throughout the 12-hour study.

On arrival at the hospital, an intravenous cannula was inserted into a forearm vein to facilitate arterialized venous blood sampling using a thermoregulated (55°C) box. A replacement cannula was inserted into the subcutaneous abdominal tissue for the variable administration of insulin lispro, rapid acting insulin analogue (Humalog; Eli Lilly, Indianapolis, IN) by an insulin pump (D-Tron; Disetronic Medical Systems, Burgdorf, Switzerland). A double-lumen catheter was inserted into the subcutaneous adipose tissue on the opposite side of the abdominal wall to extract ISF by OFM. Local skin anesthesia (Novanaest purum 2%; Gebro Broschek, Vienna, Austria) was used before the adipose tissue was cannulated. Perfusion started immediately, but sampling of the perfusate began 60 minutes after the insertion of the catheter (equilibration period) to allow the initial trauma to subside.

At the start of the study, the subjects ingested a standardised meal (40 g carbohydrate [CHO]) over 10 minutes. An individually determined prandial bolus of insulin lispro was administered at the time of meal ingestion. Only water was allowed for the rest of the study. In the case of a low PG concentration (<3.3 mmol/L) a 10- to 20-g bolus of intravenous glucose (20% dextrose solution; Fresenius Kabi, Graz, Austria) was administered.

Over 12 hours, the ISF was continuously collected and samples over 30 minutes were subjected to the determination of IG. Arterialized venous blood samples were drawn every 15 minutes for the determination of PG and every 30 minutes for the determination of plasma insulin. ISF samples and samples for the determination of plasma insulin were stored at -70°C instantly after sampling until they were analyzed. PG was determined on a bedside analyzer.

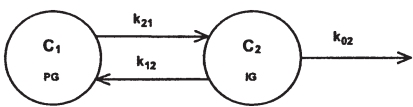


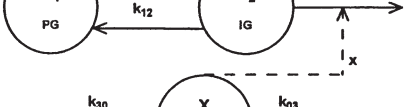
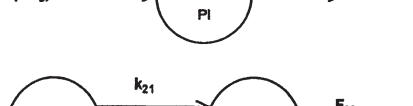
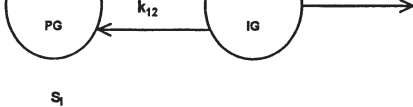
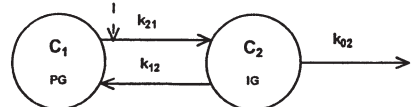
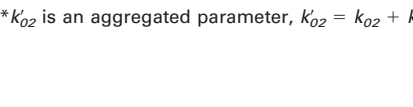
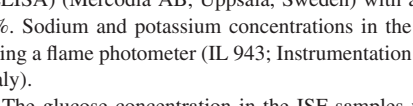
OFM

The OFM was used to obtain samples of the ISF.^{7,16} The double-lumen catheter was prepared from a conventional intravenous cannula (24 gauge \times 19 mm, 0.7 mm OD, Neoflon; Becton-Dickinson, Helsingborg, Sweden) by perforating 30 holes (0.3 mm diameter) with an Excimer Laser. The catheter was inserted into the adipose tissue of the anterior abdominal wall by a steel mandrin, which was subsequently removed and replaced by the inner cannula of the double-lumen catheter (steel tube, length 16 mm, inner diameter 0.1 mm, outer diameter 0.2 mm, Goodfellow, Cambridge, Great Britain). The inner cannula was connected to a plastic bag containing perfusate [isotonic, ion-free mannitol in aqueous solution (275 mmol/L, 288 mosmol/L); Leopold, Graz, Austria]. The perfusion fluid entered the catheter through the inner lumen and passed to the tip of the probe. Thereafter, it streamed back in the annular space between the inner cannula and the outer perforated catheter, where partial equilibration between the ISF and the perfusate occurred. The outer lumen was connected to a peristaltic pump (Minipuls 3, Gilson, France) in push-pull mode, which transported the diluted ISF effluents through the tubing system to a collecting vial on ice. The vials were sealed with a film to prevent evaporation during sampling. The flow rate was set by the peristaltic pump. To verify appropriate average flow rate, each vial was weighed before and after sampling.

Assays and Determination of IG

PG was measured in duplicate using a Beckman Glucose Analyzer 2 (Beckman Instruments, Fullerton, CA) with a coefficient of variation (CV) $<1.5\%$ of the intra-assay measurement error. Plasma insulin was measured using the Iso-Insulin enzyme-linked immunosorbent assay

Table 1. Description of Nine Proposed Compartment Models of IG Kinetics (see text for details)

Compartment Structure	Model	Equations	Comments	Parameters
	1	$dC_2/dt = k_{21}C_1 - k'_{02}C_2$	Basic linear model	k_{21}, k'_{02}^*
	2	$dC_2/dt = k_{21}C_1 - [k'_{02} - k_s(C_2 - 4.0)]C_2$	Saturable glucose removal from ISF	k_{21}, k'_{02}, k_s
	3	$dC_2/dt = k_{21}C_1 - [k'_{02} + S_1(I - I_b)]C_2$	Glucose removal from ISF linearly dependent on plasma insulin concentration	k_{21}, k'_{02}, S_1
	4	$dC_2/dt = k_{21}C_1 - k'_{02} + S_1(I - I_b) - k_s(C_2 - 4.0)]C_2$	Models 2 and 3 combined	$k_{21}, k'_{02}, k_s, S_1$
	5	$dC_2/dt = k_{21}C_1 - (X + k'_{02})C_2$ $dX/dt = k_{30}(I - I_b) - k'_{03}X$ $S_1 = k_{30}/k'_{03}$ [Eq 1]	Remote effect of insulin on glucose removal from ISF	$k_{21}, k'_{02}, S_1, k_{30}$
	6	$dC_2/dt = k_{21}C_1 - [k'_{02} + X - k_s(C_2 - 4.0)] \times C_2$ and Equation 1	Models 2 and 5 combined	$k_{21}, k'_{02}, k_s, S_1, k'_{03}$
	7	$dC_2/dt = k_{21}C_1 - k'_{02}C_2 - F_{02}$	Zero order removal of glucose from ISF	k_{21}, k'_{02}, F_{02}
	8	$dC_2/dt = [k_{21} + S_1(I - I_b)] \times C_1 - k'_{02}C_2$	Insulin effect on glucose transfer from plasma to ISF	k_{21}, k'_{02}, S_1
	9	$dC_2/dt = [k_{21} + S_1(I - I_b)] \times C_1 - k'_{02}C_2 - F_{02}$	Models 7 and 8 combined	$k_{21}, k'_{02}, F_{02}, S_1$

* k'_{02} is an aggregated parameter, $k'_{02} = k_{02} + k_{12}$.

(ELISA) (Mercodia AB, Uppsala, Sweden) with an intra-assay CV < 6%. Sodium and potassium concentrations in the ISF were measured using a flame photometer (IL 943; Instrumentation Laboratory, Milano, Italy).

The glucose concentration in the ISF samples was measured enzymatically with glucose hexokinase programmed on a Cobas Integra analyzer (Hoffman-La Roche, Basel, Switzerland). The recovery, ie, the ratio between the concentration of glucose in the sampled fluid and the concentration of glucose in the ISF, was calculated by ionic reference technique¹⁶ using Na⁺ and K⁺ ions as endogenous markers.

Data Analysis

Modelling IG kinetics. The compartment model structure was chosen to represent glucose distribution in PG and ISF (IG). The transfer of glucose between these 2 compartments represented diffusion across the capillary wall driven by the concentration gradient.¹⁷ The disposal from the IG compartment represented glucose transporters facilitated transport across the cell membrane.¹⁸

Nine models were postulated to account for the temporal variations in the IG/PG ratio. Models differed in the inclusion of physiologically motivated alterations of the 3 pathways entering/leaving the IG compartment. These effects included (1) saturable glucose disposal, (2) a zero order (constant) glucose disposal, (3) the stimulatory effect of insulin on glucose transfer from plasma to ISF, and (4) the effect of

insulin on glucose removal from ISF. In all models, PG was used as the driving function.

Model 1 was the base model and assumed time invariant fractional transfer rates from and to the IG compartment.

Model 2 assumed a saturable glucose disposal from the IG compartment. To avoid posterior identifiability problems (the situation when the precision of estimated parameters is low when a nearly identical fit is obtained with parameter values from a larger interval), the Michaelis-Menten form was not used, and the transfer rate associated with the outflux decreasing linearly with an increasing IG concentration. This is a reasonable approximation of the Michaelis-Menten form assuming that a narrow range of saturation levels is achieved during the experiment. Centering with an IG concentration of 4 mmol/L (the "basal" IG value) was used to enable comparison of parameter estimates among models.

Model 3 implemented the stimulatory effect of insulin on the glucose disposal from the IG compartment. To avoid expected posterior identifiability problems, the insulin effect did not involve a remote insulin compartment, as the infrequent sampling of IG (sample every 30 minutes) was not considered to be sufficient to determine the time delay of insulin action.

Model 4 combined models 3 and 2, ie, the stimulatory effect of insulin on glucose disposal with the effect of saturability.

Model 5 extended model 3 and used the remote insulin compartment

to assess the possibility of determining the delay in insulin action to test the assumption presented in model 3.

Model 6 combined models 5 and 2, ie, the remote insulin action on glucose disposal with the saturability effect.

Model 7 assumed that part of the glucose removed from the IG compartment is due to a zero order disposal representing a constant flux independent of the IG concentration.

Model 8 implemented a stimulatory effect of insulin on the transfer of glucose from plasma to the ISF (insulin effect on flux f_{21} in Fig 1). A remote insulin compartment was not used for posterior identifiability reasons.

Finally, model 9 combined models 7 and 8, ie, the zero order removal from the IG compartment and the stimulatory effect on the transfer of glucose from plasma to the ISF.

Formal definitions of models are shown in Table 1. The explanation of symbols is as follows: C_1 and C_2 represent PG and IG concentrations (mmol L^{-1}); k_{21} , k_{2I} , and k_{02} are transfer rate constants (min^{-1}); $k'_{02} = k_{02} + k_{12}$ is an aggregated constant (min^{-1}); k_s is the slope of saturable component of glucose disposal (min^{-1}); I is plasma insulin concentration (mU L^{-1}); I_b is basal (pre-experimental) plasma insulin concentration (mU L^{-1}); X is the remote insulin action representing the delay in insulin action (min^{-1}); k_{30} and k_{03} represent the activation and the deactivation constants of the remote insulin, respectively (min^{-2} per mU L^{-1} and min^{-1}); S_I is insulin sensitivity associated with glucose removal from IG (models 3, 4, 5, and 6) or with plasma-to-interstitial-fluid transfer (models 8 and 9) (min^{-1} per mU L^{-1}); and F_{02} is the zero order glucose disposal ($\text{mmol L}^{-1} \text{min}^{-1}$). All models are *a priori* identifiable.¹⁹

Parameter estimation. The parameters were estimated using an iterative 2-stage population analysis.^{20,21} In each iteration, model parameters were estimated using a nonlinear, weighted, least-squares algorithm with an empirical Bayesian term. Prior to the parameter estimation, parameters were log-transformed to assure non-negativity and to correct for skewed distributions of the parameters with the exception of parameter k_s which was not transformed.

Model input was PG and plasma insulin (models 3, 4, 5, 6, 8, and 9). Model output was the IG averaged over a 30-minute period.

The relative weighting, which assigns weights subject to a proportional constant, was adopted to reflect the fact that at the time of data analysis, we did not have information about the extent of the measurement error. The weight was defined as the reciprocal of the square of the nominal measurement error with a CV of 5%. The model fit error (the difference between measurements and model predictions) was determined from the nominal measurement error and the variance parameter determined by the estimation procedure.

The precision of parameter estimates was obtained from the Fisher information matrix.¹⁹ The SAAM II Population Kinetics v 1.0b software (SAAM, Seattle, WA) was used to perform the calculations.

Model identification and validation. Parameter estimates were checked for physiologic feasibility. Models with parameter estimates outside the physiologic range were excluded from further analysis. Physiologic range of parameters was determined from previously validated studies, such as that by Hovorka et al.²²

To validate the models, 3 additional criteria were adopted. These were the goodness of fit, posterior identifiability, and the distribution of residuals.¹⁹ The goodness of fit was assessed on the basis of the model fit error, ie, the distance between the measurements and the model fit. Posterior identifiability of each model was assessed on the basis of the precision of parameter estimates representing a measure of confidence associated with those estimates. A given parameter was considered nonidentifiable if the CV of the parameter estimate was $>100\%$. The Runs test evaluated the randomness of the residuals.

Model selection. The best model, ie, the model that best represented our experimental data, was selected by comparing the model fit

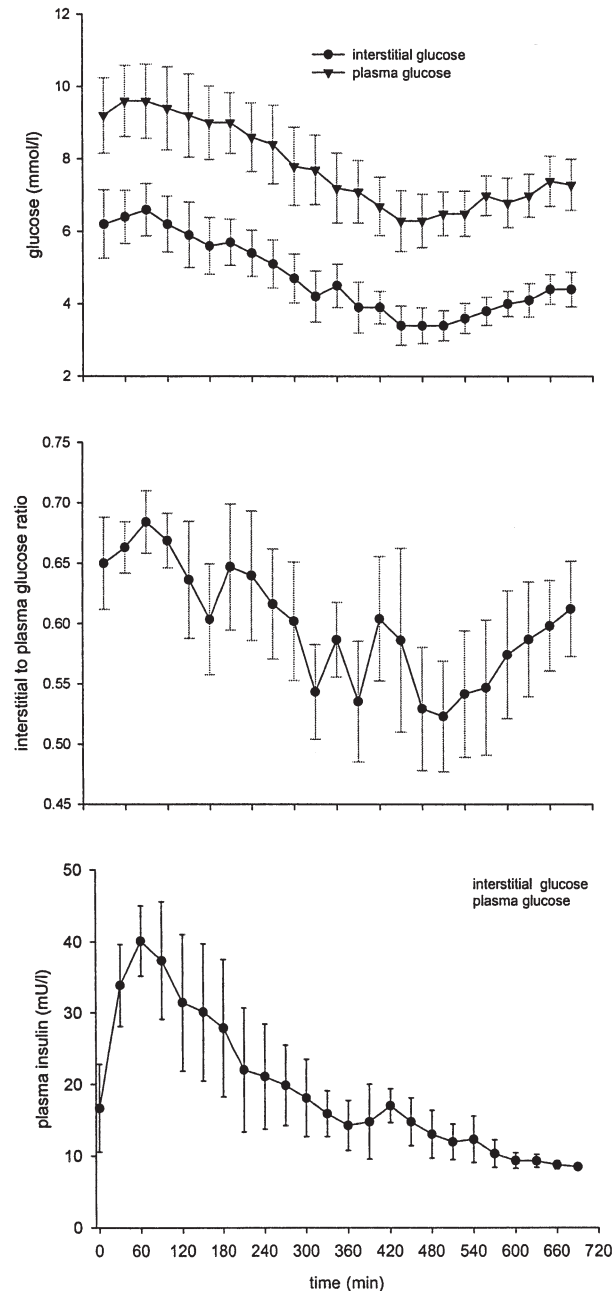


Fig 2. (A) The IG and PG concentration, (B) the IG to PG ratio, and (C) the plasma insulin concentration (mean \pm SE; $n = 9$).

error and by using the principle of parsimony as implemented by the Akaike criterion.

RESULTS

PG, IG, and Plasma Insulin

Figure 2 shows the mean PG, IG, and plasma insulin. PG and IG concentration ranged from 3.1 to 15.7 mmol/L and from 1.6 to 10.0 mmol/L, respectively. The recovery used for IG measurement ranged from 20% to 40% (data not shown). The plot also shows the IG/PG ratio (0.6 ± 0.1 ; mean \pm SD), which

Table 2. Population Analysis Results for *a posteriori* Identifiable Models

Model	k'_{02} ($10^{-2} \times \text{min}^{-1}$)	k_{21} ($10^{-2} \times \text{min}^{-1}$)	k_s ($10^{-3} \times \text{min}^{-1}$ per mmol L^{-1})	F_{02} ($10^{-2} \times \text{mmol l}^{-1} \text{min}^{-1}$)	S_1 ($10^{-4} \times \text{min}^{-1}$ per mU L^{-1})
1	8.26*	4.44 (3.82-5.15)	—	—	—
2	7.25*	4.00 (3.51-4.57)	2.4 (−1.8-6.6)	—	—
7	4.76 (1.92-11.84)	3.48 (1.41-8.60)	—	4.04 (2.17-7.52)	—
8	11.33 (5.41-23.73)	5.78 (2.43-13.76)	—	—	3.57 (1.13-11.28)
9	9.33 (4.19-20.80)	5.73 (2.30-14.26)	—	4.66 (2.12-10.26)	2.34 (0.80-6.82)

NOTE. Values are means (interquartile range) ($n = 9$).

*Individual values converged to an identical estimate.

significantly changed during the experiment ($P < .01$, 2-way analysis of variance (ANOVA) with effects due to the time instance and the subject).

Model Identification and Validation

Parameter estimate for k_{03} in model 3 (data not shown) reached very low values prolonging the time delay for the remote insulin effect (equal to the reciprocal of k_{03}) to over 350 minutes. This is equivalent to a half time of 245 minutes. Hence the insulin effect, as considered in model 3, could not be responsible for the push-pull phenomenon. The parameters for model 4, where the insulin effect was considered to be direct, could not be estimated, as the population model failed to converge. At that point, the population mean of insulin sensitivity parameter S_1 was low at $5 \times 10^{-5} \text{ min}^{-1}$ per mU L^{-1} with a very small standard deviation of approximately 10^{-8} min^{-1} per mU L^{-1} . Similarly, population models 5 and 6 failed to achieve convergence, and their parameters could not be estimated. As a result, models 3, 4, 5, and 6 were excluded from further analysis. Population parameter estimates, as determined by the iterative 2-stage parameter estimation procedure, for the remaining models are shown in Table 2. In models 1 and 2, individual estimates of k_{21} converged to an identical value indicating that the data did not contain sufficient information to discriminate this parameter individually.

Models 1, 2, 7, 8, and 9 demonstrated physiologic feasibility of parameters and posterior identifiability (see Table 3). Figure 3 shows weighted residuals associated with these models. Table 3 also shows the percentage of cases in each of the models, which passed the Runs test. The residuals are scaled assuming

a “realistic” measurement error with a CV of 10%. This is an estimate of the true measurement error, which is not known. An upper bound of 16% has been determined from samples taken simultaneously from 2 interstitial probes (data not shown).

Model Selection

The model fit error and the Akaike criterion for models 1, 2, 7, 8, and 9 are shown in Table 3. On the basis of these 2 criteria, model 9 was selected as best representing our experimental data. This model is also characterized by the highest percentage of cases that passed the Runs test.

Individual parameter estimates for model 9 are shown in Table 4. The sample model fit generated by model 9 is shown in Fig 4. The ISF equilibration time constant (delay $\tau = 1/k'_{02}$) predicted by this model was 10.7 (4.8 to 23.9) minutes [mean (interquartile range)].

DISCUSSION

Using compartment analysis, we tested for and quantified possible physiologic mechanisms related to IG kinetics during prandial, postprandial, and fasting conditions in subjects with T1DM.

Having postulated 9 distinct models, we assessed their validity on the basis of 4 criteria: physiologic feasibility, the goodness of fit, posterior identifiability, and the distribution of residuals. The selection process used the principle of parsimony and was complemented by the assessment of the residual error.

Two mechanisms have been suggested by the selected model (model 9) to explain the temporal variation in the IG/PG ratio. These are the zero order glucose removal from the ISF and an

Table 3. Summary of Validation and Model Selection Results

Model No.	Physiologic Feasibility (Yes/No)	Acceptable Precision (Yes/No)	Model Fit Error (Mean \pm SD)	Runs Test (%)*	Akaike Criterion (Mean \pm SD)
1	Yes	Yes	15 \pm 7†	11	0.97 \pm 0.38
2	Yes	Yes	13 \pm 5	56	0.91 \pm 0.30
3	No	NA	NA	NA	NA
4	No	NA	NA	NA	NA
5	No	NA	NA	NA	NA
6	No	NA	NA	NA	NA
7	Yes	Yes	11 \pm 4	44	0.80 \pm 0.28
8	Yes	Yes	10 \pm 4	56	0.72 \pm 0.35
9	Yes	Yes	9 \pm 3	67	0.71 \pm 0.26

Abbreviation: NA, not assessed.

*Percentage of cases satisfying the test.

†Expressed as fractional standard deviation (%).

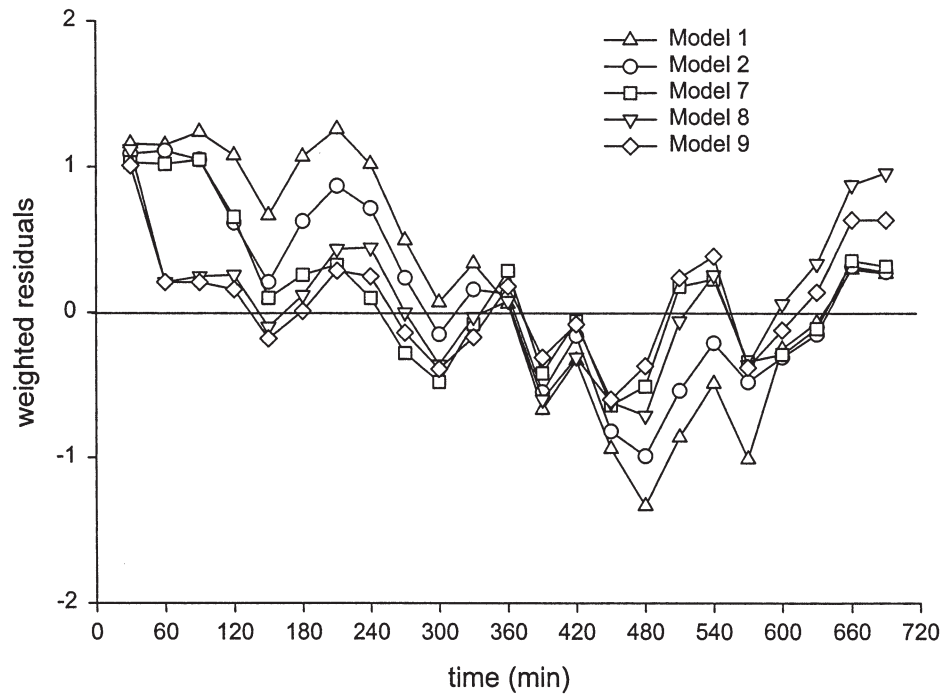


Fig 3. Weighted residuals for posterior identifiable models. Values are mean.

insulin effect on glucose transfer from the plasma to the ISF. The former implies that a portion of the disposal is constant and independent of the glucose concentration. The remaining portion is concentration dependent. At normoglycemia, the constant disposal contributes approximately 10% to the total outflux, but this relative contribution increases at lower glucose concentrations. At a hypoglycemia threshold of 3.3 mmol/L, it constitutes about 20% of the total outflux. Similarly, the IG/PG ratio is also glucose dependent. For example, a decrease in PG from 9 to 3.3 mmol/L will reduce the IG/PG ratio by 0.1. Extrapolating the results outside the range of our experimental data, a more pronounced decrease from 9 to 2 mmol/L would lower the IG/PG ratio even further, ie, by 0.2. This finding is consistent with observations made by others, who also found a decrease in IG/PG ratio in the hypoglycemic range,^{15,23} and the finding may have important implications on the calibration of ISF glucose sensors.

Table 4. Parameter Estimates for Best Model 9

Subject	k'_{02} ($10^{-2} \times \text{min}^{-1}$)	k_{21} ($10^{-2} \times \text{min}^{-1}$)	F_{02} ($10^{-2} \times \text{mmol/L}$)	S_i ($10^{-4} \times \text{min}^{-1}$ per mU/L)
1	21.15 (66)*	8.93 (61)	4.18 (111)	15.5 (70)
2	10.09 (49)	6.30 (48)	12.31 (55)	5.6 (58)
3	22.81 (58)	15.81 (57)	2.33 (113)	0.5 (146)
4	0.65 (31)	0.24 (16)	0.56 (71)	0.3 (45)
5	7.18 (30)	5.55 (29)	2.32 (67)	0.4 (138)
6	10.45 (48)	7.91 (49)	18.15 (53)	2.1 (141)
7	23.32 (39)	15.33 (39)	4.19 (77)	12.6 (53)
8	8.59 (23)	6.97 (22)	10.18 (25)	3.0 (33)
9	11.22 (55)	6.51 (52)	8.52 (75)	4.4 (72)

*Precision of parameter estimate expressed as a fractional standard deviation (%).

Several investigators have noted that recovery from hypoglycemia takes longer in IG compared with PG.^{14,15,23,24} This is normally attributed to the push-pull phenomenon, ie, the insulin-stimulated IG disposal. However, our data offer an alternative explanation. The zero order disposal affects the time-to-equilibrium in IG due to the kinetic properties of model 9 (see model equations). An increase in glucose is associated with a prolonged time-to-equilibrium, whereas a decrease in glucose is associated with a shorter equilibration time.

The constant disposal can be explained by a portion of glucose transport across the adipose cell membrane being sat-

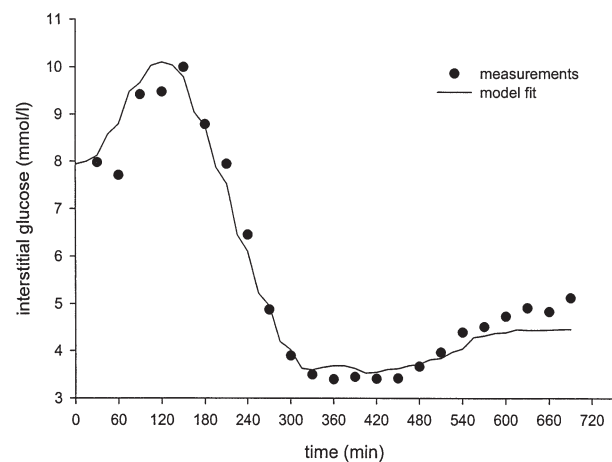


Fig 4. An example of an individual fit (in subject 8) generated by best model 9.

urated even at low glucose concentrations as supported by Kozka et al,²⁵ who found low K_M value of 3.6 mmol/L and low glucose transport activity in human adipose tissue with low GLUT4 abundance, GLUT4 being the principal glucose transporter isoform in human adipose cells.¹⁷

The second mechanism suggested by the present study is the stimulatory effect of insulin on glucose transfer from the plasma to the ISF. Contrary to current views, this suggests that the IG/PG ratio increases in parallel with plasma insulin within its physiologic range. The effect is modest. The IG/PG ratio increases only by 0.03 per 10 mU/L of plasma insulin with a considerable between subject variability. One should emphasize here the failure of models 3 to 5, which were not compatible with the experimental data. The long time delay of insulin action estimated by model 3 (350 minutes) shifted the insulin action from the early peak into a period of low plasma insulin concentrations making this model behave as model 8.

Two possible explanations for this effect are at hand. Insulin has been found to induce vasodilatation^{26,27} and also to mediate capillary recruitment in tissues.²⁸ Both of these effects potentially improve the microvascular perfusion and may be responsible for the insulin-stimulated transfer of glucose from the plasma to the ISF.

Similarly to Rebrin et al,¹³ our study was not able to detect the stimulatory effect of insulin on glucose disposal, so called the push-pull phenomenon, which has been reported by others and widely discussed in the literature.^{11,14,15} The pull part of the push-pull phenomenon occurs when the (insulin-stimulated) enhanced uptake of IG by the adipocytes is not fully compensated for by increased delivery of glucose from the plasma. The phenomenon has been documented in studies using high physiologic/supraphysiologic insulin concentrations during a hyperinsulinemic clamp, whereas plasma insulin concentrations in our study remained in the low physiologic range potentially explaining the discrepancy and questioning the relevance of the push-pull phenomenon in physiologic conditions. Furthermore, studies in humans showed that while glucose transport in the adipose tissue of healthy lean subjects is stimulated by insulin approximately 2-fold, the transport in the adipose tissue of obese or overweight subjects is not responsive to insulin.²⁹ This is also relevant to the present study, in which some subjects were on the borderline of obesity.

The IG/PG ratio estimated by model 9 is 0.56 at PG of 9 mmol/L. It is reduced to around 0.46 at the hypoglycemic threshold of 3.3 mmol/L. This is consistent with other studies. Monsod et al¹⁵ documented the IG/PG ratio of 0.65 under basal glucose and insulin levels and also documented a decrease in the IG/PG ratio by approximately 20% when moving from euglycemia to hypoglycemia. Schaupp et al¹⁶ reported a ratio in the range 0.60 to 0.75 within the PG range from 5 to 10 mmol/L. Both studies investigated healthy subjects.

The equilibration time constant reported in the literature varies considerably from 2 minutes¹¹ to 25 minutes,²⁴ and even 45 minutes,¹² but most investigators report a range from 5 to 10 minutes,^{10,11,13,30} which is comparable to the equilibration time constant obtained in this study (11 minutes). There are, however, difficulties in making direct comparisons as the differences may arise from the use of different sampling techniques, different glucose/insulin ranges, and different subject categories.

The identifiable models, models 1, 2, 7, 8, and 9, provided consistent parameter estimates (see Table 2). The transfer rate constants k'_{02} and k_{21} compare well between the models. However, the individual parameter estimates varied considerably between subjects (see Table 4). Other investigators also reported high between subject variability.³¹

The selected model 9 was only marginally better than model 7 and model 8 (see Table 2). It failed the Runs test in 3 of 9 cases, suggesting the influence of additional unmodelled effects on the IG/PG ratio, such as variable recovery or hormonal influences on model parameters. As hormones are cyclical in nature, we proposed a model in which oscillations were superimposed on the transfer rate constant k_{02} . Preliminary results showed a marked improvement in the model fit and a higher number of cases passing the Runs test. However, we excluded the model from detailed reporting as the nature of the oscillations is lacking explicit physiologic interpretation.

Diabetes management can greatly benefit from subcutaneous glucose monitoring. This presumes that subcutaneous sensing devices provide clinically relevant information such as hypo- and hyperglycemia alerts. The calibration of glucose sensors is critical in this respect. Normally, 1 to 2 PG values within a relatively narrow range would be expected to calibrate the sensor for the use during real-time glucose sensing. Extrapolating the calibration curve outside the observed range assumes a certain relationship between plasma and IG. The present results suggest that a calibration curve is not proportional and that it should include a component due to the zero order glucose disposal. This should improve the sensitivity and specificity of the sensor especially in the hypoglycemia range, when the use of a proportional calibration curve may result in spurious nocturnal hypoglycemia readings as observed with the continuous glucose monitoring system sensor.³² However, the considerable interindividual differences in the IG/PG kinetics suggest that an individualization of the calibration relationship might further improve the sensor performance.

In conclusion, we developed and quantified a model of IG kinetics applicable to physiologic conditions in subjects with T1DM. The model implements 2 effects, which are responsible for temporal variations in the IG/PG ratio, the zero order removal of glucose from the ISF and the insulin-stimulated glucose transfer from the plasma to the ISF.

REFERENCES

1. Robinson MR, Eaton RP, Haaland DM, et al: Noninvasive glucose monitoring in diabetic patients—A preliminary evaluation. *Clin Chem* 38:1618-1622, 1992
2. Heise HM: Non-invasive monitoring of metabolites using near infrared spectroscopy: State of the art. *Horm Metab Res* 28:527-534, 1996
3. Schmidt FJ, Slatter WJ, Schooner AJM: Glucose concentration in subcutaneous extracellular space. *Diabetes Care* 16:695-700, 1993
4. Fischer U, Ertle R, Rebrin K, et al: The wick technique—A reference method for implanted glucose sensors. *Artif Organs* 13:453-457, 1989. 1987
5. Bolinder J, Ungerstedt U, Arner P: Long-term continuous glucose

monitoring with microdialysis in ambulatory insulin-dependent diabetic-patients. *Lancet* 342:1080-1085, 1993

6. Tamada JA, Bohannon NJV, Potts RO: Measurement of glucose in diabetic subjects using noninvasive transdermal extraction. *Nat Med* 1:1198-1201, 1995

7. Trajanoski Z, Brunner GA, Schaupp L, et al: Open-flow microperfusion of subcutaneous adipose tissue for on-line continuous ex vivo measurement of glucose concentration. *Diabetes Care* 20:1114-1121, 1997

8. Schaupp L, Brunner GA, Schaller H, et al: Glucose monitoring in the adipose tissue of type 1 diabetic patients using open-flow microperfusion and microdialysis. *Diabetologia* 44:A46, 2001 (abstr)

9. Claremont DJ, Sambrook IE, Penton C, et al: Subcutaneous implantation of a ferrocene-mediated glucose sensor in pigs. *Diabetologia* 29:817-821, 1986

10. Bantle JP, Thomas W: Glucose measurement in patients with diabetes mellitus with dermal interstitial fluid. *J Lab Clin Med* 130:436-441, 1997

11. Sternberg F, Meyerhoff C, Mennel FJ, et al: Does fall in tissue glucose precede fall in blood glucose? *Diabetologia* 39:609-612, 1996

12. Pfeiffer EF, Meyerhoff C, Bischof F, et al: On line continuous monitoring of subcutaneous tissue glucose is feasible by combining portable glucosensor with microdialysis. *Horm Metab Res* 25:121-124, 1993

13. Rebrin K, Steil GM, Van Antwerp WP, et al: Subcutaneous glucose predicts plasma glucose independent of insulin: Implications for continuous monitoring. *Am J Physiol* E561-E571, 1999

14. Aussedat B, Dupire-Angel M, Gifford R, et al: Interstitial glucose concentration and glycemia: Implications for continuous subcutaneous glucose monitoring. *Am J Physiol* 278:E716-E728, 2000

15. Monsod TP, Flanagan DE, Rife F, et al: Do sensor glucose levels accurately predict plasma glucose concentrations during hypoglycemia and hypoinsulinemia. *Diabetes Care* 25:889-893, 2002

16. Schaupp L, Ellmerer M, Brunner GA, et al: Direct access to interstitial fluid in adipose tissue in humans by use of open-flow microperfusion. *Am J Physiol* 39:E401-E408, 1999

17. Zierler K: Whole body glucose metabolism. *Am J Physiol* 276:E409-E426, 1999

18. Mueckler M: Facilitative glucose transporters. *Eur J Biochem* 219:713-725, 1994

19. Carson ER, Cobelli C, Finkelstein L: *The Mathematical Modeling of Metabolic and Endocrine Systems* (ed 1). New York, NY, Wiley, 1983

20. Steimer JL, Mallet A, Golmard JL, et al: Alternative approaches to estimation of population pharmacokinetic parameters: Comparison with the nonlinear mixed-effect model. *Drug Metab Rev* 15:265-292, 1984

21. Hovorka R, Vicini P: Parameter estimation. in: Carson ER, Cobelli C, (eds): *Modelling Methodology for Physiology and Medicine*. San Diego, CA, Academic, 2001, pp 107-151

22. Hovorka R, Shojae-Moradie F, Carroll PV, et al: Partitioning glucose distribution/transport, disposal, and endogenous production during IVGTT. *Am J Physiol* 282:E992-E1007, 2002

23. Kerr D, Cheyne EH, Weiss M, et al: Accuracy of Minimed continuous glucose monitoring system during hypoglycaemia. *Diabetologia* 44:A239, 2001 (abstr)

24. Moberg E, HagstromToft E, Arner P, et al: Protracted glucose fall in subcutaneous adipose tissue and skeletal muscle compared with blood during insulin-induced hypoglycaemia. *Diabetologia* 40:1320-1326, 1997

25. Kozka JJ, Clark AE, Reckless JPD, et al: The effects of insulin on the level and activity of the GLUT4 present in human adipose-cells. *Diabetologia* 38:661-666, 1995

26. Scherrer U, Randin D, Vollenweider P, et al: Nitric-oxide release accounts for insulins vascular effects in humans. *J Clin Invest* 94:2511-2515, 1994

27. Steinberg HO, Brechtel G, Johnson A, et al: Insulin-mediated skeletal muscle vasodilation is nitric oxide dependent. A novel action of insulin to increase nitric oxide release. *J Clin Invest* 94:1172-1179, 1994

28. Serne EH, IJzerman RG, Gans ROB, et al: Direct evidence for insulin-induced capillary recruitment in skin of healthy subjects during physiological hyperinsulinemia. *Diabetes* 51:1515-1522, 2002

29. Stolic M, Russell A, Hutley L, et al: Glucose uptake and insulin action in human adipose tissue—Influence of BMI, anatomical depot and body fat distribution. *Int J Obes* 26:17-23, 2002

30. Rebec MV, Neal DW, Farmer B, et al: Comparison of plasma and interstitial fluid glucose obtained by microperforation. *Diabetes* 51:A11, 2002 (abstr)

31. Summers LKM, Clark ML, Humphreys SM, et al: The use of microdialysis to monitor rapid changes in glucose concentration. *Horm Metab Res* 31:424-428, 1999

32. McGowan K, Thomas W, Moran A: Spurious reporting of nocturnal hypoglycemia by CGMS in patients with tightly controlled type I diabetes. *Diabetes Care* 25:1499-1503, 2002